

## Morphology and Stability of Growing Multiwall Carbon Nanotubes

Young-Kyun Kwon,<sup>1</sup> Young Hee Lee,<sup>1,2</sup> Seong-Gon Kim,<sup>1,\*</sup> Philippe Jund,<sup>1,†</sup>  
David Tománek,<sup>1</sup> and Richard E. Smalley<sup>3</sup>

<sup>1</sup>*Department of Physics and Astronomy, Michigan State University,  
East Lansing, Michigan 48824-1116*

<sup>2</sup>*Department of Physics and Semiconductor Physics Research Center,  
Jeonbuk National University, Jeonju 561-756, Korea*

<sup>3</sup>*Center for Nanoscale Science and Technology, and Departments of Chemistry and Physics,  
Rice University, P.O. Box 1892, Houston, Texas 77251  
(Received 29 April 1997)*

We use *ab initio* and parametrized calculations to investigate the morphology and structural stability at the growing edge of multiwall carbon nanotubes. We find that these open-ended structures are stabilized against dome closure by strong covalent bonds connecting the exposed edges of adjacent walls. Growth at the open edge involves rearrangement of these bonds, which are mediated by carbon atoms bridging the gap and change the tip morphology significantly. Presence of a strong “lip-lip” interaction can explain formation of carbon nanotubes under annealing conditions. [S0031-9007(97)04056-8]

PACS numbers: 61.48.+c, 61.50.Ah, 68.70.+w, 81.10.Aj

Since the first observation of nanotubes in the carbon arc [1,2], their formation mechanism has been traditionally associated with external factors such as strong electric fields [1–6], presence of hydrogen atoms [7–9], catalytic metal particles [10–17], or a surface at low temperature [18,19]. Successful synthesis of nanotubes by laser vaporization of pure carbon [20] raises the question why such tubular structures often prevail over their more stable spherical counterparts [21–27]. It is furthermore intriguing that these nanotubes, even though grown under annealing conditions, are very long and defect-free, appear to be rather inert, and—unless grown in presence of a metal catalyst—always have multiple walls.

Observation of the rather unstable carbon tubes under annealing conditions suggests the presence of an efficient mechanism that prevents their closure by a dome [20,28]. In the case of single-wall nanotubes, metal atoms are believed to perform this task by catalytically removing pentagon defects at the edge [16,17]. In the absence of such a catalyst or spatial anisotropy (e.g., due to an electric field [1]), formation of pentagon defects must be prevented at the growing edge of a multiwall tube.

In this Letter, we present the first microscopic study of the preferential growth mechanism of multiwall nanotubes. Our results elucidate not only the stable morphologies at the reconstructed edge of growing multiwall “armchair” and “zigzag” tubes, but also the detailed dome closure mechanism terminating the growth. We find that carbon atoms adsorbing at the growing edge often prefer to bridge the gap between adjacent wall edges by covalent bonds, rather than to saturate dangling bonds at the edge of individual walls.

The *ab initio* calculations are performed using the cluster code DMol [29,30], based on the density functional formalism within the local density approximation (LDA).

In the double-numerical basis set [29], the C 2s and C 2p orbitals are represented by two wave functions each, and 3d type wave functions are used to describe polarization. We use the frozen core approximation to treat the inner core electrons and the von Barth and Hedin exchange-correlation potential [31]. Since a full structure optimization of long open-ended nanotubes is not tractable using *ab initio* techniques, we guided our search by a parametrized linear combination of atomic orbitals (LCAO) method. This computationally efficient  $O(N)$  approach [32] has been previously used with success to describe the formation energetics [33] and disintegration dynamics [34] of fullerenes.

Here, we consider two examples of achiral double-wall nanotubes, shown in Fig. 1. The (5,5)@(10,10) tube [Fig. 1(a)] consists of concentric tubes with armchair edges, and the (9,0)@(18,0) tube [Fig. 1(b)] contains tubes with zigzag edges [35]. The equilibrium C-C distance in these tubes is very close to the graphite value  $d_{CC} = 1.42 \text{ \AA}$ . The radii of the inner tubes,  $R(5,5) = 3.42 \text{ \AA} \approx R(9,0) = 3.57 \text{ \AA}$ , and the outer tubes,  $R(10,10) = 6.78 \text{ \AA} \approx R(18,0) = 7.06 \text{ \AA}$ , are very similar for the armchair and the zigzag systems. The interwall distance of  $\approx 3.4 \text{ \AA}$  is close to the graphite value [1,2].

During the growth process, carbon atoms can adsorb at the open edge of either tube, or connect these edges by a bridging covalent bond. The structure can be characterized by the type of the inner and outer tube, the mutual tube orientation, and the arrangement of the adatoms. Let us first consider the exposed edge of the double-armchair (AA) (5,5)@(10,10) nanotube. Selected optimized tube-edge structures are shown in Fig. 1(a). Different structures at the tip were generated by adding  $N_{\text{add}} = 10$  carbon atoms in various positions at both tube ends. A global unrestricted optimization was performed using the LCAO

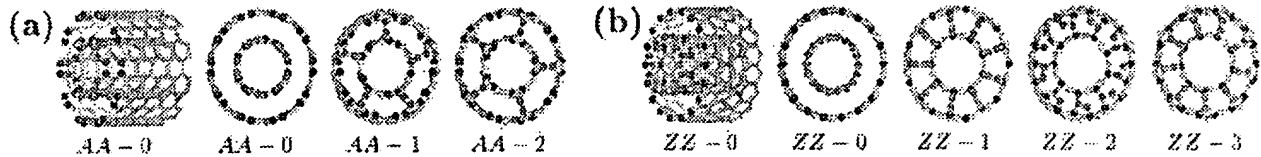


FIG. 1(color). Relaxed geometries at the growing edge of achiral double-wall carbon nanotubes. (a) The (5,5)@(10,10) armchair double tube, with no lip-lip interaction (structure AA-0, in perspective and end-on view), and with lip-lip interaction (structures AA-1 and AA-2). (b) The (9,0)@(18,0) zigzag double tube, with similar radii as the armchair system. Shown are structures with no lip-lip interaction (ZZ-0, in perspective and end-on view), and with lip-lip interaction (ZZ-1, ZZ-2, and ZZ-3). Inner-tube atoms are shown in green, exposed edge atoms in blue, and the added atoms in red.

method. Only the topmost two layers, in addition to the adatoms, were relaxed in the corresponding LDA calculations.

When constructing the reference structure AA-0, we let the extra carbon atoms saturate the dangling bonds at the inner tube. There is no interaction between the adjacent walls in this open structure. Placing the extra atoms radially between the two exposed edges in the AA-1 structure gains the system  $\Delta E = -0.42$  eV per extra carbon atom when the structure is fully relaxed. Stabilizing “lip-lip” interactions have been previously postulated based on chemical intuition supported by parametrized calculations [20,28], and on molecular dynamics simulations [36]. The large energy gain in the AA-1 structure and the short bond length  $d_a = 1.33$  Å (1.31 Å from LDA) of the dimer bridging the gap indicate that the lip-lip interaction is mediated by a strong covalent bond. Restricting the relaxation to the two topmost layers at the tube end reduced the energy gain per extra carbon atom to  $\Delta E = -0.37$  eV, which is very close to the LDA value  $\Delta E = -0.25$  eV. Also the geometry optimized within LDA is virtually indistinguishable from that based on the LCAO calculation.

We find that not all possible covalent bonds between adjacent tube edges stabilize the system with respect to the AA-0 structure. The energy difference per added atom  $\Delta E = +3.52$  eV for the AA-2 structure, shown in Fig. 1(a), suggests that this structure is unlikely to form. To understand the stability gain of the AA-1 and stability loss of the AA-2 double tubes with respect to the AA-0 structure, we show the color-coded binding energies of individual atoms at the relaxed edge in Fig. 2. Bright colors indicate that it is only atoms at the outermost tube edge that are less bound than atoms in the tube interior, which are nearly as stable as in graphite. Energy gain of the AA-1 structure results from one of the added atoms closing a pentagon at the outer edge, thus gaining stability for itself and its neighbors at the outer edge. We find that also the inner lip atoms are stabilized, but to a lesser degree. Figure 2 also indicates that it is the unstable triangles at the edge which destabilize the AA-2 structure.

Qualitatively similar results are obtained for the double-zigzag (ZZ) (9,0)@(18,0) nanotube. Different tip morphologies are generated by placing 18 extra carbon atoms in different positions at either tube end. The geometries of globally optimized structures are shown in Fig. 1(b).

In analogy to the armchair case, we construct the reference structure ZZ-0 by placing extra carbon atoms only at the edge of the inner tube, as shown in Fig. 1(b). While there is no connection between adjacent tube edges in the ZZ-0 structure, such an interaction can be established by placing extra carbon atoms in between the two exposed edges. As in the case of armchair double-wall tubes, not all such lip-lip interaction topologies are energetically favorable. In the ZZ-1 structure, radially arranged adatoms saturate the dangling bonds at the exposed edges, thereby gaining the system  $\Delta E = -0.25$  eV per extra carbon atom with respect to the reference structure ZZ-0. Similar to the situation at the AA-1 tube end, we find the added dimer to connect the edges by a strong covalent bond of length  $d_a = 1.28$  Å (1.26 Å from LDA). In the even more favorable edge morphology ZZ-2, with an azimuthal arrangement of the extra atoms, the system gains  $\Delta E = -0.54$  eV per extra carbon atom with respect to ZZ-0 when the structure is fully relaxed. The azimuthal orientation of the dimer allows it to saturate dangling bonds at both edges. In contrast to the favorable ZZ-1 and ZZ-2 morphologies, the ZZ-3 structure is less stable by  $\Delta E = +0.67$  eV than the ZZ-0 reference structure, since it contains squares at the outer edge. Because of energetic preference of rigid

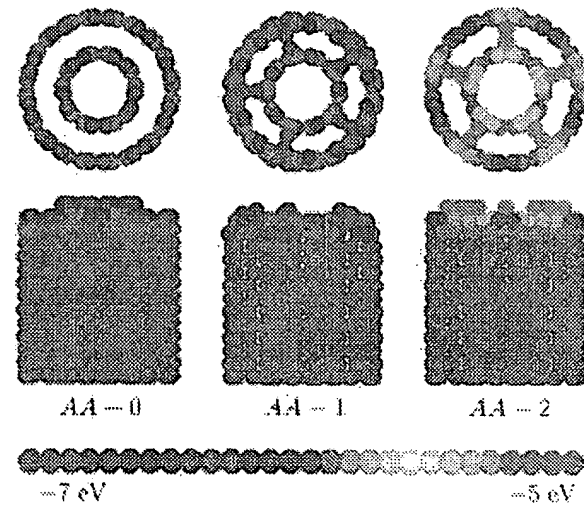


FIG. 2(color). Color-coded binding energy of individual atoms in the optimized AA-0, AA-1, and AA-2 nanotubes, described in Fig. 1, in end-on and side view.

covalent bonds connecting exposed edges of adjacent walls, we do not expect individual tubes to rotate independently in nested multiwall nanotubes.

To analyze the growth process of multiwall tubes, we extend two concepts used in discussions of crystal surface growth to nanotube edges. For a growing nanotube, we define the edge coverage by  $\Theta = N_{\text{add}}/N_e$ . Here,  $N_{\text{add}}$  is the number of added atoms and  $N_e$  is the number of edge atoms, which is the same as the number of atoms in any layer of the nanotube. Next, we define the edge energy by

$$E_e = [E_{b,\text{tot}}(C_N \text{ nanotube}) - NE_b(C_\infty \text{ nanotube})]/N_e, \quad (1)$$

which is independent of coverage. In this equation,  $E_{b,\text{tot}}(C_N \text{ nanotube})$  is the total binding energy of the truncated nanotube, and  $E_b(C_\infty \text{ nanotube})$  is the binding energy per atom in an infinite nanotube. Hence, low  $E_e$  values correspond to stable edge morphologies.

Optimum edge morphologies and the associated energetics [37] for a growing (5,5)@(10,10) double tube are shown in Fig. 3. The stable AA-1 structure, shown in Fig. 1(a) and discussed above, corresponds to a coverage of  $\Theta = 1/3$  and an edge energy of  $E_e = 0.80 \text{ eV}$ . This structure can be further stabilized by adsorbing five extra carbon dimers at either tube end, as shown in Fig. 3(a). This increases the coverage to  $\Theta = 2/3$ , but reduces the

edge energy to  $E_e = 0.56 \text{ eV}$ , which is significantly lower than the value  $E_e = 0.92 \text{ eV}$  in absence of the lip-lip interaction. Structures optimized for a given coverage of the growing double tube are shown in Fig. 3(a) and the corresponding edge energies in Fig. 3(b). We note that the most stable structures contain hexagons and pentagons, but no squares or triangles. Since the function of the covalent lip-lip interactions is to saturate dangling bonds at the edge, the bridging atoms continuously move with the growing edge. As the coverages  $\Theta = 0$  and  $\Theta = 2$  correspond to the same tube, all information relevant for continuous growth is contained in the coverage interval  $0 < \Theta \leq 2$  described here.

Tube growth is driven by the total energy gained when carbon from the atmosphere adsorbs at the growing tube end. Since under synthesis conditions [20] the carbon atmosphere consists to a large degree of linear structures, we associate the total energy gain  $\Delta E(\Theta)$  with the conversion of carbon atoms in chains, with a binding energy  $E_b = -6.05 \text{ eV}$  [32], to a coexisting, growing (5,5)@(10,10) double tube. The result, shown in Fig. 3(c), indicates that in spite of edge energy fluctuations depicted in Fig. 3(b), tube growth is a strongly exothermic process.

Finally we consider the energetics of dome closure that terminates the growth process. The inner and outer tubes of the (5,5)@(10,10) system can be closed perfectly by hemispheres of the  $C_{60}$  and  $C_{240}$  fullerenes, respectively. Starting from the double-tube structure described by  $\Theta = 2$ , complete dome closure requires a coverage increase by  $\Delta\Theta \geq 2\frac{2}{3}$  to  $\Theta = 4\frac{2}{3}$  in our case. The edge energy for the case that the inner and outer tubes begin closing by noninteracting domes (i.e., no lip-lip interaction) is shown by + and the dotted line in Figs. 3(b) and 3(c). Only selected structures of the closing dome, such as for  $\Theta = 4\frac{1}{6}$ , can be further stabilized by a lip-lip interaction, which lowers the edge energy by as much as  $\Delta E_e = -0.13 \text{ eV}$  to  $E_e(\Theta = 4\frac{1}{6}) = 0.53 \text{ eV}$  (□ and dash-dotted line). As the stabilizing lip-lip bonds have to be disrupted completely for the dome closure to continue, the system encounters substantial energy barriers during this process. Since the edge energy is higher for a closing dome than for a continually growing tube ( $\diamond$  and dashed line), especially in the range  $2.5 < \Theta < 3.0$  corresponding to initiation of the dome closure, spontaneous termination of growing tubes is unlikely to occur.

These results have multiple, experimentally verifiable consequences. Our main claim is that sustained growth of defect-free carbon nanotubes is closely linked to efficiently preventing the formation of pentagon defects which would cause a premature dome closure. For one, this is due to the covalent connection between adjacent nanotube walls at the growing edge which reduces the likelihood of such defects forming at either edge. Another reason is that saturation of dangling bonds by lip-lip interactions at the growing open edge should substantially reduce the growth rate, thus leaving more time for defects to heal out and yielding perfect tubes.

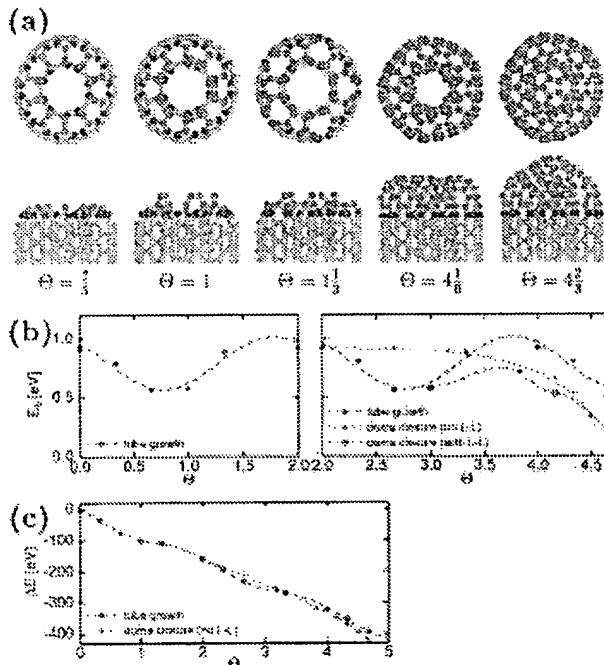


FIG. 3(color). (a) Optimum geometry at the growing edge of (5,5)@(10,10) nanotube, as a function of edge coverage  $\Theta$ . The color code is the same as in Fig. 1. (b) Edge energy  $E_e$  as a function of coverage for the energetically favored growth and dome closure mode of the nanotube. (c) Total energy gain  $\Delta E$  for the nanotube coexisting with an infinite carbon chain, during its growth and dome closure process with and without lip-lip (L-L) interactions.

One immediate consequence of postulating covalent lip-lip interactions as indispensable for tube growth in a pure carbon atmosphere is that all such nanotubes should have multiple walls [20]. Without the passivating "spot welds," single-wall tubes are prone to being etched away in the aggressive atmosphere under synthesis conditions, which explains their absence in the tube material. The presence of covalent spot welds in chiral multiwall tubes, on the other hand, is also expected to prevent their "catastrophic burn-back" by "unraveling" in extremely high electric fields [38,39].

One can easily imagine other growth scenarios than the double-wall mechanism discussed above, which yields only even-walled nanotubes. Covalent spot welds, simultaneously connecting an exposed edge to adjacent wall edges on the inner and outer sides, can yield odd-walled nanotubes. Simple bond-counting arguments suggest that it is more difficult to saturate all dangling bonds at the edge of odd-walled tubes, thus reducing their stability and inertness. This may explain the apparent abundance of nanotubes with an even number of walls [20].

Since the stability of particular lip-lip interactions depends mainly on the local geometry, we expect our results to hold also for tubes with different radii or chiralities. Our model does not imply that the growth of multiwall nanotubes proceeds in the optimized and orderly fashion discussed in Fig. 3, or that only specific achiral tubes may profit from the lip-lip interaction. We realize that the nanotube structure, whether chiral or achiral, is determined early on during the formation of the tube nucleus. Each favorable covalent bond connecting the exposed tube edges, however, will lower the edge energy and hence stabilize the tip, making it less prone to defect formation. The resulting passivation of the tube end slows down, but does not stop the tube growth. The strained structure at the tube tip invites preferential carbon adsorption at the growing edge. As the carbon coverage increases, the tube end will undergo a complex, concerted exchange of atoms leading to the most stable tip structure. Such structures have all been discussed above, and involve covalent lip-lip interactions. It appears unlikely that occasional spot welds could remain intact as the tip position advances, since such defects would locally decrease the stability and inertness of the otherwise perfect graphitic tubes. Hence we expect net growth of perfect tubes to result from carbon accretion at the exposed edge, involving lip-lip interactions only at the growing end of the intermediate structures.

One of us (D.T.) gratefully acknowledges the hospitality of the Rice Quantum Institute and financial support by the National Science Foundation under Grant No. PHY-92-24745 when this work was initiated. One of us (Y.H.L.) acknowledges financial support by the Korea Science and Engineering Foundation (KOSEF) (Grant No. KOSEF94-0501-11) and partial support by the Semiconductor Physics Research Center at Jeonbuk National University and the Office of Naval Research under Grant No. N00014-90-J-1396.

\*Present address: Code 6690, Complex Systems Theory Branch, Naval Research Laboratory, Washington, DC 20375-5320.

<sup>†</sup>Present address: Laboratoire des Verres, Université de Montpellier 2, Case 069-Place Eugène Bataillon, F-34095, Montpellier Cedex 5, France.

- [1] S. Iijima, *Nature (London)* **354**, 56 (1991).
- [2] For a general review, see T. W. Ebbesen, *Phys. Today* **49**, No. 6, 26 (1996).
- [3] R. E. Smalley, *Mater. Sci. Eng. B* **19**, 1 (1993).
- [4] Y. Saito *et al.*, *Chem. Phys. Lett.* **204**, 277 (1993).
- [5] T. W. Ebbesen, *Annu. Rev. Mater. Sci.* **24**, 235 (1994).
- [6] A. Maiti *et al.*, *Phys. Rev. Lett.* **73**, 2468 (1994).
- [7] M. Endo *et al.*, *J. Phys. Chem. Solids* **54**, 1841 (1993).
- [8] N. Hatta and K. Murata, *Chem. Phys. Lett.* **217**, 398 (1994).
- [9] J. B. Howard *et al.*, *Nature (London)* **370**, 603 (1994).
- [10] S. Iijima and T. Ichihashi, *Nature (London)* **363**, 603 (1993).
- [11] D. S. Bethune *et al.*, *Nature (London)* **363**, 605 (1993).
- [12] S. Amelinckx *et al.*, *Science* **265**, 635 (1994).
- [13] V. Ivanov *et al.*, *Chem. Phys. Lett.* **223**, 329 (1994).
- [14] M. J. Yacaman *et al.*, *Appl. Phys. Lett.* **62**, 202 (1993).
- [15] Ching-Hwa Kiang *et al.*, *J. Phys. Chem.* **98**, 6612 (1994).
- [16] A. Thess *et al.*, *Science* **273**, 483 (1996).
- [17] Young Hee Lee *et al.*, *Phys. Rev. Lett.* **78**, 2393 (1997).
- [18] M. Ge and K. Sattler, *Appl. Phys. Lett.* **65**, 2284 (1994); *Chem. Phys. Lett.* **220**, 192 (1994); *Appl. Phys. Lett.* **64**, 710 (1994); *Science* **260**, 515 (1993).
- [19] L. A. Chernozatonskii *et al.*, *Chem. Phys. Lett.* **228**, 94 (1994).
- [20] Ting Guo *et al.*, *J. Phys. Chem.* **99**, 10 694 (1995).
- [21] D. Ugarte, *Nature (London)* **359**, 707 (1992); *Europhys. Lett.* **22**, 45 (1993).
- [22] Gary B. Adams *et al.*, *Science* **256**, 1792 (1992).
- [23] D. Tománek *et al.*, *Phys. Rev. B* **48**, 157461 (1993).
- [24] A. Maiti *et al.*, *Phys. Rev. Lett.* **70**, 3023 (1993).
- [25] D. H. Robertson *et al.*, *Phys. Rev. B* **45**, 12 592 (1992).
- [26] X. F. Zhang *et al.*, *J. Cryst. Growth* **130**, 368 (1993).
- [27] S. Amelinckx *et al.*, *Science* **267**, 1334 (1995).
- [28] David Tománek, in *Large Clusters of Atoms and Molecules*, edited by T.P. Martin, NATO ASI Series Vol. 313 (Kluwer Academic Publishers, Dordrecht, The Netherlands, 1996), p. 405.
- [29] B. Delley, *J. Chem. Phys.* **92**, 508 (1990).
- [30] DMol is a registered software product of Molecular Simulations Inc.
- [31] U. von Barth and L. Hedin, *J. Phys. C* **5**, 1629 (1972).
- [32] W. Zhong *et al.*, *Solid State Commun.* **86**, 607 (1993).
- [33] David Tománek and Michael A. Schlüter, *Phys. Rev. Lett.* **67**, 2331 (1991).
- [34] Seong Gon Kim and David Tománek, *Phys. Rev. Lett.* **72**, 2418 (1994).
- [35] M. S. Dresselhaus, G. Dresselhaus, and P.C. Eklund, *Science of Fullerenes and Carbon Nanotubes* (Academic, San Diego, 1996).
- [36] J.-C. Charlier *et al.*, *Science* **275**, 646 (1997).
- [37] Since there is no absolute guarantee that a given structure is the globally most stable tube isomer, the presented edge energies should be considered as upper bounds for  $E_\epsilon$ .
- [38] A. G. Rinzler *et al.*, *Science* **269**, 1550 (1995).
- [39] Young Hee Lee *et al.*, *Chem. Phys. Lett.* **265**, 667 (1997).